Published in final edited form as:
J Am Chem Soc. 2010 June 9; 132(22): 7645–7655. doi:10.1021/ja910290c.

Computation-Guided Development of Au-Catalyzed Cycloisomerizations Proceeding via 1,2-Si- or 1,2-H Migrations: Regiodivergent Synthesis of Silylfurans

Alexander S. Dudnik[§], **Yuanzhi Xia**[†,‡], **Yahong Li**[*,†,‡], and **Vladimir Gevorgyan**[*,§]

[§]Department of Chemistry, University of Illinois at Chicago, Chicago, Illinois 60607

[†]Key Laboratory of Organic Synthesis of Jiangsu Province, Department of Chemistry and Chemical Engineering, Suzhou University, Suzhou 215006, China

[‡]Key Laboratory of Salt Lake Resources and Chemistry of Chinese Academy of Sciences, Qinghai Institute of Salt Lakes, Xining 810008, China

Abstract

A novel highly efficient regiodivergent Au-catalyzed cycloisomerization of allenyl- and homopropargylic ketones into synthetically valuable 2- and 3-silylfurans has been designed with the aid of the DFT calculations. This cascade transformation features 1,2-Si- or 1,2-H migrations in a common Au-carbene intermediate. Both experimental and computational results clearly indicate that the 1,2-Si migration is kinetically favored over the 1,2-shifts of H, alkyl, and aryl groups in the β-Si-substituted Au-carbenes. In addition, experimental results on the Au(I)-catalyzed cycloisomerization of homopropargylic ketones demonstrated that counterion and solvent effects could reverse the above migratory preference. The DFT calculations provided a rationale for this 1,2-migration regiodivergency. Thus, in the case of $AuSbF_6^-$, DFT-simulated reaction proceeds through the initial propargyl-allenyl isomerization followed by the cyclization into the Au-carbene intermediate with the exclusive formation of 1,2-Si migration products and solvent effects cannot affect this regioselectivity. However, in the case of TfO^--counterion, reaction occurs via the initial 5-*endo-dig* cyclization to give cyclic furyl-Au intermediate. In the case of nonpolar solvents, subsequent ipso-protiodeauration of the latter is kinetically more favorable than the generation of the common Au-carbene intermediate and leads to the formation of formal 1,2-H migration products. In contrast, when polar solvent is employed in this DFT-simulated reaction, β-to-Au protonation of the furyl-Au species to give Au-carbene intermediate competes with the ipso-protiodeauration. Subsequent dissociation of the triflate ligand in this carbene in polar media due to efficient solvation of charged intermediates facilitates formation of the 1,2-Si shift products. The above results of DFT calculations were validated by the experimental data. The present study demonstrates that the DFT calculations could efficiently support experimental results, providing guidance for rational design of new catalytic transformations.

Keywords

furans; gold; rearrangement; allenes; alkynes; DFT calculations

liyahong@suda.edu.cn; vlad@uic.edu.

Supporting Information Available: Computational and experimental details, and full citation of computational methods. This material is available free of charge via the Internet at http://pubs.acs.org.

Introduction

Cycloisomerizations of alkynes and allenes arguably represent the most versatile methodologies for the assembly of heterocycles.[1] Introduction of molecular rearrangements into these processes often provides highly efficient routes toward densely substituted heterocycles. Within this area, Hashmi[2] and later Che[3] reported Au-catalyzed[4] cycloisomerizations of alkynyl- and allenyl ketones into furans.[5] These cascades were proposed to proceed via a formation of the key putative Au-carbene **1** followed by a formal 1,2-H shift (Scheme 1).[6] Apparently, 1,2-migration of groups other than H, proceeding via intermediate **1**, would allow for an expedient synthesis of diversely functionalized furans with substitution patterns not easily accessible via the existing methodologies.[7] Along this line, we recently reported the Au-catalyzed regiodivergent synthesis of halofurans involving 1,2-Hal or 1,2-H migration in **1**.[7j] Herein, we wish to report a computation-designed regiodivergent Au-catalyzed cycloisomerization of homopropargyl- and allenyl ketones into silylfurans, featuring 1,2-Si- or 1,2-H migration in the Au-carbene intermediate **1** (Scheme 2).

Results and Discussion

Recent DFT study revealed that the Au-catalyzed cycloisomerization of bromoallenyl ketones[7j] proceeds through the Au-carbene **1**, wherein the 1,2-Br migration is kinetically favored over a facile 1,2-H shift.[8] Naturally, we were interested in identifying other migrating groups capable of undergoing a selective 1,2-migration over the 1,2-H shift. Thus, we turned our attention to a silyl group, which is known to undergo a facile 1,2-migration to electron-deficient centers. Despite the well-known 1,2-Si migration to cationic centers,[9,10] only little attention was devoted to 1,2-Si shifts to free-[11] or metal-stabilized carbenes,[12] especially with a focus on synthetic significance. Besides, scarce studies on migratory aptitudes in these systems have been reported.[11,12]

We envisioned that DFT calculations could shed light on the relative rates of 1,2-migrations of Si-, Hand alkyl groups in the Au-carbene **1'** (Scheme 3).[13] Thus, the results of DFT computations[14,15] indicated that the 1,2-Si migration is strongly favored over the 1,2-shifts of methyl, phenyl, and even H in **1'** for both $AuCl_3$ and H_3PAu^+ (Scheme 3).[14]

Synthesis of Furans via Au(III)-Catalyzed 1,2-Si Migration in Allenes

It occurred to us that the Au-catalyzed cyclization of silyl allenes **4** could provide a straightforward access to the Au-carbene **1'** via a well-established route (eq 1).[2,6] The latter intermediate, upon the 1,2-Si shift, should furnish the 3-silylfuran **2**.

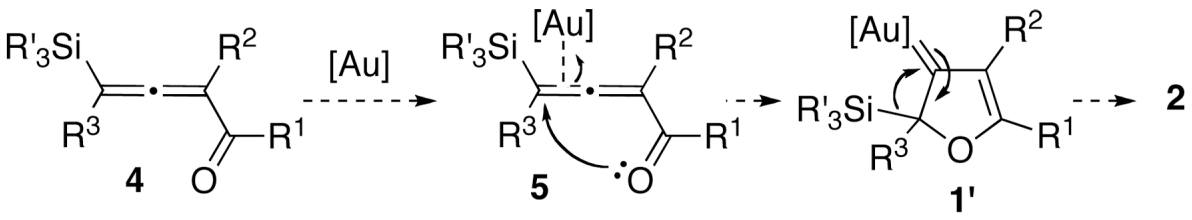

(1)

To this end, we have tested the possible cycloisomerization of allenes **4** into 3-silylfurans **2** in the presence of various Au catalysts. Gratifyingly, it was found, that α-to-Si alkyl-substituted allenes **4a** and **4b** in the presence of $AuCl_3$-catalyst underwent a highly selective 1,2-Si migration, affording 3-silylfurans **2a** and **2b** in high yields (Table 1, entries 1–2). Likewise,

cycloisomerization of phenyl-substituted allenes **4c,d** proceeded highly efficiently to give 3-silylfurans **2c,d** as sole isomers (entries 3–4). To our delight, α-to-Si-unsubstituted allene **4e** cyclized highly selectively into a product of the exclusive 1,2-Si- over 1,2-H shift **2e** in both toluene or more polar, nitromethane, solvent (entry 5). Thus, the experimentally observed exclusive Si-migration is in an excellent agreement with the computation-predicted higher 1,2-migratory aptitude of Si- over H-, Alk-, and Ar groups. It is worth mentioning, that allene **4e** was not stable in the presence of $Ph_3PAuOTf$ complex when performing reaction in toluene or 1,2-dichloroethane (DCE) solvents. In addition, similarly to $AuCl_3$, employment of $Ph_3PAuSbF_6$ catalyst provided exclusive formation of 1,2-Si migration product **2e** in DCE solvent, albeit notable amounts of the desilylated 3-methyl-2-phenylfuran were observed.

The computed energy surface for the Au-catalyzed cycloisomerization of allene **4** ($AuCl_3$) is provided in Scheme 4.[14] Hence, a highly exergonic (24.7 kcal/mol) cyclization of complex **4-AuCl$_3$** into the carbene **1-AuCl$_3$** required 2.6 kcal/mol activation energy only. A subsequent kinetically more favorable 1,2-Si migration (**TS1_2-AuCl$_3$**, 11.1 kcal/mol activation energy) over the 1,2-H shift (**TS1_3-AuCl$_3$**, 23.6 kcal/mol activation energy) led to the product complex **2-AuCl$_3$**. A requisite ligand exchange reaction proceeded as illustrated in Scheme 5 to complete the catalytic cycle, thus furnishing the final products and regenerating the active allene complex **4-AuCl$_3$**. The free energy values indicated that the formation of **2** and **3** via the reactions of allene **4** with **2-AuCl$_3$** and **3-AuCl$_3$** were both endergonic by 17.8 and 12.2 kcal/mol, respectively (Scheme 5). The optimized structures of key stationary points along the reaction pathway for the cycloisomerization of allenes **4** are presented in Figure 1.

Counterion Effects on the Au(I)-Catalyzed 1,2-Si Migration in Alkynes

Next, we envisioned that easily accessible homopropargylic ketones **6** could also serve as precursors[7e,7j] for the allene **5** toward the common Au-carbene intermediate **1** (eq 2). Alternatively, cyclization of **6** into furyl-Au species **7**,[2,16] followed by its β-protonation at the vinyl-gold moiety[17] would generate the Au-carbene **1**. Based on the computation results, it was predicted that a subsequent facile 1,2-Si shift in **1** would furnish 3-silylfuran **2**. On the other hand, counterion-assisted[8,18] 1,2-H shift in **1** or direct α-protonation of the vinyl-Au moiety in **7** might compete with the 1,2-Si migration, affording the 2-silylfurans **3** (eq 2).

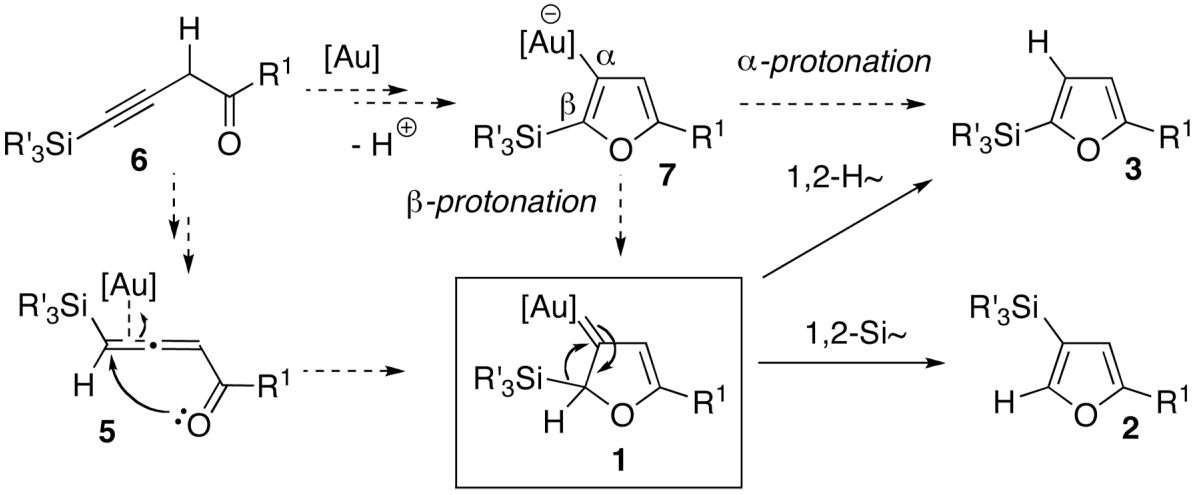

(2)

Thus, DFT calculations were performed to evaluate possible counterion effects[8,18] and establish overall reaction pathways for cycloisomerization of homopropargylic ketones **6** in the presence of electrophilic $Ph_3PAuOTf$ and $Ph_3PAuSbF_6$ catalysts in DCE or toluene solvents, respectively. The potential energy surfaces for the predictions of the effects of TfO^-- and SbF_6^--counterions are depicted in Schemes 6 and 7, respectively. In the case of $Ph_3PAuOTf$ catalyst in DCE solution (Scheme 6), a highly exergonic (21.3 kcal/mol) direct 5-*endo-dig* cyclization of complex **T-C** proceeded with the simultaneous abstraction of propargylic H-atom by TfO^--counterion to give the furyl-Au **T-IN1** and HOTf, requiring 10.9 kcal/mol activation energy. Subsequent endergonic association of HOTf (15.1 kcal/mol) with the α-C-atom of the vinyl-Au moiety in **T-IN1** followed by ipso-protiodeauration of the **T-IN2** intermediate (**T-TS4**, 4.9 kcal/mol activation energy) provided product of the formal 1,2-H migration **T-3**. On the other hand, kinetically more favorable β-protonation at the vinyl-gold moiety in **T-IN2** (**T-TS2**, 4.7 kcal/mol activation energy) over the ipso-protiodeauration (**T-TS4**, 4.9 kcal/mol activation energy) should lead to a competing generation of the Au carbene **T-1**. Subsequent 1,2-Si migration from **T-1** required 10.7 kcal/mol free energy (**T-TS3**) to give 1,2-Si migration product **T-2**. Alternatively, it was found that TfO^- ligand dissociation reaction could occur efficiently from carbene **T-1** (6.0 kcal/mol) to give more electrophilic carbene **C-1**, wherein a more kinetically facile 1,2-Si shift (**C-TS1**, 10.1 kcal/mol activation energy) afforded 3-silylfuran **C-2**. In both carbene intermediates **T-1** and **C-1**, direct 1,2-H migrations were predicted to have higher activation energy barriers, than those for direct 1,2-Si shifts (**C-TS2** versus **C-TS1**, 22.3 versus 10.1 kcal/mol activation free energy, respectively). In addition, an alternative reaction pathway, involving generation of reactive allene-Au complex **T-5** via $Ph_3PAuOTf$-assisted propargyl-allenyl isomerization of **T-C** was found to be higher in energy (**T-TS6**, 16.4 kcal/mol) than the direct cyclization route in DCE. Thus, based on the predicted 0.2 kcal/mol difference between α- (**T-TS4**) and β- (**T-TS2**) protonation paths, a competing formation of products **2** and **3** can be expected in the $Ph_3PAuOTf$-catalyzed cycloisomerization of homopropargylic ketone **6**. It should be mentioned that analogous high-energy profiles were later found for the propargyl-allenyl isomerization of **6** into **5** and for the direct 1,2-H shift in Au-carbene intermediates **1** in toluene solvent (*vide infra*). The optimized structures of key stationary points along the reaction pathway for the $Ph_3PAuOTf$-catalyzed cycloisomerization of alkynes **6** are presented in Figure 2.

In the case of $Ph_3PAuSbF_6$ catalyst (Scheme 7) in DCE solvent, direct 5-*endo-dig* cyclization of complex **H-C** afforded cyclic zwitter-ionic intermediate **H-IN1** via the **H-TS1** transition state, requiring 10.8 kcal/mol activation free energy. However, we were not able to locate the next transition state for the highly endergonic (23.6 kcal/mol) formation of the furyl-Au intermediate **T-IN1** and $HSbF_6$, probably due to an extreme acidity of $HSbF_6$. An alternative pathway, involving a [1,5]-hydride shift via **H-TS2**, was also found to be high in energy (22.2 kcal/mol activation free energy). We believe that an extremely high acidity of $HSbF_6$ and very low nucleophilicity of its conjugate base SbF_6^- complicate DFT-simulation of the elementary reaction processes involving a counterion-assisted proton transfer step. This reasoning prompted us to perform DFT-calculations of the $Ph_3PAuSbF_6$-catalyzed reaction in the presence of three water molecule cluster $(H_2O)_3$, which could model reactivity of a more nucleophilic than SbF_6^- counterion and much milder than $HSbF_6$ acid in its monoprotonated form. Accordingly, initial coordination of water cluster to homopropargylic ketone **H-C** provided **HW-C1** endergonically (10.4 kcal/mol free energy).[8,13h] Similarly to TfO^--counterion, water cluster could also abstract propargylic H-atom during a subsequent 5-*endo-dig* cyclization of **HW-C1** (**HW-TS1**, 9.1 kcal/mol activation free energy) to give the furyl-Au **HW-IN1** and protonated water cluster.[19] However, a lower energy reaction path was found for the complex **HW-C1**. Thus, formation of the activated allene **H-5** from the latter occurred as a stepwise H-abstraction/donation process via transition states **HW-TS4** and **HW-TS5**, respectively. The first step of this process required an activation free energy of only 3.9 kcal/mol in DCE and 2.9 kcal/mol in toluene, respectively, leading to the intermediate **HW-IN2**

exergonically. The second quite facile H-donation step to give **HW-5** occurred with the activation energies of 7.3 kcal/mol (DCE) or 8.4 kcal/mol (toluene) and was followed by exergonic decoordination of water cluster to produce allene-Au complex **H-5**. A facile cyclization of the latter via **H-TS3** provided Au-carbene **H-1** with 5.3 kcal/mol activation free energy in DCE and 4.9 kcal/mol in toluene. A subsequent 1,2-Si migration in **H-1** via **H-TS4** was strongly favored over the 1,2-H shift (**H-TS5**) in both DCE and toluene solvents, leading to the 1,2-Si migration product complex **H-2**. The optimized structures of key stationary points along the reaction pathway for the $Ph_3PAuSbF_6$-catalyzed cycloisomerization of alkynes **6** are presented in Figure 3.

To examine the above DFT-based prognosis, we investigated cycloisomerization of the homopropargylic ketones **6** in the presence of various Au catalysts (Table 2). It was found that the experimental results overall are in good agreement with the computational predictions.[14] Thus, the Au-catalyzed cycloisomerization of alkynes **6** in the presence of non-nucleophilic SbF_6^--counterion in DCE gives exclusive formation of 1,2-Si migration products **2f, l**, and **k** (entries 1, 7, 11). As suggested by the DFT-calculations, switching to $Ph_3PAuOTf$ catalyst in DCE with a more nucleophilic counterion leads to a competing formation of 1,2-Si- and 1,2-H migration products **2f** and **3f**, respectively, for the cycloisomerization of **6f** (entry 2). However, the DFT predictions cannot explain a selective formation of the 1,2-Si migration product **2l** during the cycloisomerization of **6l** (entry 10). In addition, it was found that $AuCl_3$ could also catalyze cycloisomerization of alkynes **6**, however, the regioselectivity of this reaction toward the 1,2-Si migration product **2f** was poor in a variety of solvents (entries 4–6). Unfortunately, analogous study on counterion effect in allenyl systems was not possible since allenes **4** were not stable in the presence of $Ph_3PAuOTf$ and even less electrophilic $Ph_3PAuOBz$ complexes.

Solvent Effects on the Au(I)-Catalyzed 1,2-Si Migration in Alkynes

Remarkably, it was found that the solvent effect could dominate over the counterion effect, as evidenced by a reverse regioselectivity observed in the $Ph_3PAuOTf$-catalyzed cycloisomerization of **6** (Table 2, entries 2 vs 3 and 9 vs 10).[20] Accordingly, when reaction was conducted in DCE solution, the preferred formation of 1,2-Si migration products was observed. However, when toluene was employed as a solvent, the 1,2-H migration products were the major ones. To shed light on these quite uncommon results,[20] DFT calculations for evaluation of the solvent effects on the 1,2-H and 1,2-Si migrations were performed. DFT predictions for the $Ph_3PAuOTf$-catalyzed reaction in DCE solvent were provided above (Scheme 6). The results for toluene solvent are outlined in Scheme 8. According to the calculated potential energy surfaces, employment of toluene solvent leads to the intermediate **T-IN2** via 5-*endo-dig* cyclization of **T-C** with a reaction energy profile similar to that for DCE solvent. However, in the case of toluene solvent, there is no difference in activation energy barriers for α- (**T-TS4**) and β- (**T-TS4**) protonation pathways of furyl-Au complex **T-IN2**. Most importantly, while solvents do not affect the relative barriers of the subsequent 1,2-H- and 1,2-Si migrations from Au-carbene intermediates **T-1** or **C-1** much, they alter the stability of the dissociated noninteracting Au-carbene **C-1** and TfO^--anion relative to the associated Au-carbene complex **T-1**. For instance, when the reaction is conducted in toluene solution, which has a lower polarity than DCE, the stabilization effects of the solvent on the charged species **C-1** and TfO^- are limited (compare relative energies of **C-1** intermediates in Schemes 6 and 8). On the other hand, an alternative direct 1,2-Si migration from carbene **T-1** via **T-TS3** has 10.7 kcal/mol activation free energy barrier. Since complex **T-1** does not undergo dissociation of the TfO^--ligand in toluene solution easily, its formation becomes reversible, forcing reaction to proceed via the α-protonation route **T-IN2** – **T-TS4** – **T3**, which is 3.9 kcal/mol lower in activation free energy than the direct 1,2-Si shift in **T-1**. The DFT calculations suggest that the $Ph_3PAuOTf$-catalyzed cycloisomerization of **6** in toluene solvent should lead

to the 1,2-H migration product **3**, thus supporting the experimentally observed reversed regioselectivity of the reaction (Table 2, entries 2 vs 3 and 9 vs 10). In contrast to the above case, no solvent effect was observed in the DFT-simulated $Ph_3PAuSbF_6$-catalyzed reactions (Scheme 7). Thus, formation of the allene-Au complex **H-5** and its cyclization into the Au-carbene **H-1** were found to be more efficient than other possible processes in both DCE and toluene solvents. In addition, energies of the direct- or base-/SbF_6^--assisted 1,2-H migrations were much higher than that of the 1,2-Si migration from **H-1**, regardless on the solvent (compare entries 7 and 8 in Table 2). Thus, the experimentally observed migratory preference (Table 2, entries 1, 7, 8, and 11) for the $Ph_3PAuSbF_6$-catalyzed reactions was in a good agreement with the performed DFT calculations. Finally, it is worth mentioning here that, in contrast to the cycloisomerization of alkynes **6**, employment of solvents more polar than toluene did not affect the $AuCl_3$-catalyzed cycloisomerization of allenyl ketone **4e** (Table 1, entry 5).

Synthesis of Furans via Au(I)-Catalyzed 1,2-Si Migration in Alkynes

Next, we investigated the scope of the above 1,2-Si migration cascade reaction of alkynes (Table 3). Thus, cycloisomerization of a variety of 4-silyl homopropargylic ketones **6**, possessing aryl- (entries 1, 2), primary- (entries 7–9), and tertiary (entry 6) alkyl groups, proceeded smoothly affording the C2-unsubstituted 3-silylfurans **2** as sole regioisomers in good to excellent yields (Table 3). It was found that alkynes bearing TMS- (entries 1–7), TES- (entry 8), as well as $PhMe_2Si$ (entry 9) groups could be successfully employed in this transformation. In the case of cycloisomerization of substrates **6** bearing electron-deficient aryl substituents (entries 3–5), 1,2-H shift competed with the 1,2-Si-migration, which resulted in formation of isomeric silylfurans **2** and **3** with good to high degrees of regioselectivity favoring 3-silylfurans **2**. It was also demonstrated that a variety of functional groups such as methoxy (entry 2), bromo (entry 3), cyano (entry 4), and nitro (entry 5) could be tolerated under these reaction conditions.

Conclusion

In summary, we developed a regiodivergent Au-catalyzed cycloisomerization of allenyl- and homopropargylic ketones into 2- and 3-silylfurans featuring 1,2-Si- or 1,2-H migrations in the common Au-carbene intermediate. The present methodology constitutes a general and efficient route for the synthesis of 3-silylfurans, important synthons,[21] not easily available via the existing methodologies. Both experimental and computational results indicate that the 1,2-Si migration is kinetically more favored over the 1,2-shifts of H, alkyl-, and aryl groups in the β-Si-substituted Au-carbenes. However, according to the experimental data obtained for the cycloisomerization of homopropargylic ketones, counterion and solvent effects may reverse this migratory preference. The DFT calculations provided a rationale for this 1,2-migration regiodivergency. Accordingly, in the case of cationic Au-catalyst possessing non-nucleophilic SbF_6^--counterion, DFT-simulated reaction affords 1,2-Si migration products exclusively via the initial propargyl-allenyl isomerization followed by the cyclization into the Au-carbene intermediate regardless on the solvent employed in the reaction. However, in the case of TfO^--counterion in nonpolar solvents, a pronounced counterion effect is observed. Thus, reaction occurs via the initial 5-*endo*-*dig* cyclization to give cyclic furyl-Au intermediate followed by a subsequent ipso-protiodeauration, which is kinetically more favorable than the generation of the common Au-carbene intermediate and leads to the formation of formal 1,2-H migration products. In contrast, when polar solvent is employed, β-to-Au protonation of the furyl-Au species, leading to Au-carbene intermediate, competes with the ipso-protiodeauration. Subsequent dissociation of the triflate ligand in the latter carbene in polar media due to efficient solvation facilitates formation of the 1,2-Si shift products. The above results of DFT calculations were validated by the experimental data. Finally, the present study highlights that the DFT calculations could efficiently complement experimental results,

providing guidance for design of new transformations and offering better understanding of this chemistry.

Supplementary Material

Refer to Web version on PubMed Central for supplementary material.

Acknowledgments

This work was supported by Hundreds of Talents Program of CAS, Natural Science Foundation of China (20872105), and NIH of the US (GM-64444).

References

1. For selected reviews on transition metal-catalyzed transformations of alkynes and allenes, see: (a) Alonso F, Beletskaya IP, Yus M. Chem. Rev 2004;104:3079. [PubMed: 15186189] (b) Kirsch SF. Synthesis 2008:3183. (c) Nakamura I, Yamamoto Y. Chem. Rev 2004;104:2127. [PubMed: 15137788] (d) Patil TN, Yamamoto Y. Chem. Rev 2008;108:3395. [PubMed: 18611054] (e) Jiménez-Núñez E, Echavarren AM. Chem. Commun 2007:333. (f) Crone B, Kirsch SF. Chem. Eur. J 2008;14:3514. (g) Rubin M, Sromek AW, Gevorgyan V. Synlett 2003:2265. (h) Ma S. Chem. Rev 2005;105:2829. [PubMed: 16011326] (i) Bates RW, Satcharoen V. Chem. Soc. Rev 2002;31:12. [PubMed: 12108979] (j) Zimmer R, Dinesh CU, Nandanan E, Khan FA. Chem. Rev 2000;100:3067. [PubMed: 11749314] (k) Abu Sohel SM, Liu R-S. Chem. Soc. Rev 2009;38:2269. [PubMed: 19623349] (l) Majumdar KC, Debnath P, Roy B. Heterocycles 2009;78:2661.

2. Hashmi ASK, Schwarz L, Choi J-H, Frost TM. Angew. Chem. Int. Ed 2000;39:2285.

3. Zhou CY, Chan PWH, Che CM. Org. Lett 2006;8:325. [PubMed: 16408906]

4. For selected recent reviews on Au-chemistry, see: (a) Arcadi A. Chem. Rev 2008;108:3266. [PubMed: 18651778] (b) Hashmi ASK. Chem. Rev 2007;107:3180. [PubMed: 17580975] (c) Gorin DJ, Toste FD. Nature 2007;446:395. [PubMed: 17377576] (d) Li Z, Brouwer C, He C. Chem. Rev 2008;108:3239. [PubMed: 18613729] (e) Fürstner A, Davies PW. Angew. Chem., Int. Ed 2007;46:3410. (f) Jiménez-Núñez E, Echavarren AM. Chem. Rev 2008;109:3326. (g) Widenhoefer RA, Han X. Eur. J. Org. Chem 2006:4555. (h) Shen HC. Tetrahedron 2008;64:3885. (i) Shen HC. Tetrahedron 2008;64:7847. (j) Hashmi ASK, Hutchings GJ. Angew. Chem., Int. Ed 2006;45:7896. (k) Belmont P, Parker E. Eur. J. Org. Chem 2009:6075. (l) Hoffmann-Röder A, Krause N. Org. Biomol. Chem 2005;3:387. [PubMed: 15678171]

5. For recent reviews on furan synthesis, see: (a) Brown RCD. Angew. Chem., Int. Ed 2005;44:850. (b) Kirsch SF. Org. Biomol. Chem 2006;4:2076. [PubMed: 16729118] (c) Patil NT, Yamamoto Y. ARKIVOC 2007:121. (d) Hou XL, Cheung HY, Hon TY, Kwan PL, Lo TH, Tong SY, Wong HNC. Tetrahedron 1998;54:1955. (e) Hou X-L, Yang Z, Yeung K-S, Wong HNC. Prog. Heterocycl. Chem 2008;19:176. (f) Balme G, Bouyssi D, Monteiro N. Heterocycles 2007;73:87. (g) D'Souza DM, Muller TJJ. Chem. Soc. Rev 2007;36:1095. [PubMed: 17576477] For selected recent examples on transition metal-catalyzed synthesis of furans, see: (h) Zhang M, Jiang H-F, Neumann H, Beller M, Dixneuf PH. Angew. Chem., Int. Ed 2009;48:1681. (i) Xiao Y, Zhang J. Adv. Synth. Catal 2009;351:617. (j) Pan Y-M, Zhao S-Y, Ji W-H, Zhan Z-P. J. Comb. Chem 2009;11:103. [PubMed: 19046075] (k) Zhang G, Huang X, Li G, Zhang L. J. Am. Chem. Soc 2008;130:1814. [PubMed: 18205360] (l) Xiao Y, Zhang J. Angew. Chem., Int. Ed 2008;47:1903. (m) Shibata Y, Noguchi K, Hirano M, Tanaka K. Org. Lett 2008;10:2825. [PubMed: 18543939] (n) Ji K-G, Shen Y-W, Shu X-Z, Xiao H-Q, Bian Y-J, Liang Y-M. Adv. Synth. Catal 2008;350:1275. (o) Barluenga J, Riesgo L, Vicente R, López LA, Tomás M. J. Am. Chem. Soc 2008;130:13528. [PubMed: 18800797] (p) Aurrecoechea JM, Durana A, Pérez E. J. Org. Chem 2008;73:3650. [PubMed: 18363372] (q) Zhao L-B, Guan Z-H, Han Y, Xie Y-X, He S, Liang Y-M. J. Org. Chem 2007;72:10276. [PubMed: 18041850] (r) Shu X-Z, Liu X-Y, Xiao H-Q, Ji K-G, Guo L-N, Qi C-Z, Liang Y-M. Adv. Synth. Catal 2007;349:2493. (s) Peng L, Zhang X, Ma M, Wang J. Angew. Chem., Int. Ed 2007;46:1905. (t) Arimitsu S, Hammond GB. J. Org. Chem 2007;72:8559. [PubMed: 17910507] (u) Zhang J, Schmalz H-G. Angew. Chem., Int. Ed 2006;45:6704. (v) Aponick A, Li C-Y, Malinge J, Marques EF. Org. Lett 2009;11:4624. [PubMed: 19772313] (w) Blanc A, Tenbrink K, Weibel J-M, Pale P. J. Org. Chem 2009;74:5342. [PubMed: 19572586] (x) Blanc

A, Tenbrink K, Weibel J-M, Pale P. J. Org. Chem 2009;74:4360. [PubMed: 19400569] (y) Yoshida M, Al-Amin M, Shishido K. Synthesis 2009:2454. (z) Egi M, Azechi K, Akai S. Org. Lett 2009;11:5002. [PubMed: 19780532] (aa) Liu F, Yu Y, Zhang J. Angew. Chem., Int. Ed 2009;48:5505. (ab) Suhre MH, Reif M, Kirsch SF. Org. Lett 2005;7:3925. [PubMed: 16119933] (ac) Patil NT, Wu H, Yamamoto Y. J. Org. Chem 2005;70:4531. [PubMed: 15903340] (ad) Liu Y, Song F, Song Z, Liu M, Yan B. Org. Lett 2005;7:5409. [PubMed: 16288518] (ae) Yao T, Zhang X, Larock RC. J. Am. Chem. Soc 2004;126:11164. [PubMed: 15355093] (af) Hashmi ASK, Sinha P. Adv. Synth. Catal 2004;346:432. (ag) Kel'in AV, Gevorgyan V. J. Org. Chem 2002;67:95. [PubMed: 11777444]

6. For Ag-catalyzed synthesis of furans via a formal 1,2-H shift in allenones, see: (a) Marshall JA, Robinson ED. J. Org. Chem 1990;55:3450. (b) Hashmi ASK. Angew. Chem., Int. Ed. Engl 1995;34:1581.
7. For selected examples on 1,2-shifts in the synthesis of aromatic heterocycles, see: (a) Kim JT, Kel'in AV, Gevorgyan V. Angew. Chem., Int. Ed 2003;42:98. (b) Sromek AW, Kel'in AV, Gevorgyan V. Angew. Chem., Int. Ed 2004;43:2280. (c) Schwier T, Sromek AW, Yap DML, Chernyak D, Gevorgyan V. J. Am. Chem. Soc 2007;129:9868. [PubMed: 17658805] (d) Dudnik AS, Gevorgyan V. Angew. Chem., Int. Ed 2007;46:5195. (e) Dudnik AS, Sromek AW, Rubina M, Kim JT, Kel'in AV, Gevorgyan V. J. Am. Chem. Soc 2008;130:1440. [PubMed: 18173272] (f) Gorin DJ, Davis NR, Toste FD. J. Am. Chem. Soc 2005;127:11260. [PubMed: 16089452] (g) Li G, Huang X, Zhang L. Angew. Chem., Int. Ed 2008;47:346. (h) Takaya J, Udagawa S, Kusama H, Iwasawa N. Angew. Chem., Int. Ed 2008;47:4906. (i) Davies PW, Martin N. Org. Lett 2009;11:2293. [PubMed: 19425591] (j) Sromek AW, Rubina M, Gevorgyan V. J. Am. Chem. Soc 2005;127:10500. [PubMed: 16045332]
8. Xia Y, Dudnik AS, Gevorgyan V, Li Y. J. Am. Chem. Soc 2008;130:6940. [PubMed: 18461941]
9. For selected examples, see: (a) Danheiser RL, Carini DJ, Basak A. J. Am. Chem. Soc 1981;103:1604. (b) Danheiser RL, Kwasigroch CA, Tsai Y-M. J. Am. Chem. Soc 1985;107:7233. (c) Becker DA, Danheiser RL. J. Am. Chem. Soc 1989;111:389. (d) Panek JS, Yang M. J. Am. Chem. Soc 1991;113:9868.
10. For selected examples of Si-shifts in the synthesis of aromatic heterocycles, see: (a) Nakamura I, Sato T, Terada M, Yamamoto Y. Org. Lett 2007;9:4081. [PubMed: 17784768] (b) Seregin IV, Gevorgyan V. J. Am. Chem. Soc 2006;128:12050. [PubMed: 16967938] (c) Danheiser RL, Stoner EJ, Koyama H, Yamashita DS, Klade CA. J. Am. Chem. Soc 1989;111:4407.
11. (a) Creary X, Butchko MA. J. Org. Chem 2001;66:1115. [PubMed: 11312937] (b) Creary X, Wang Y-X. Tetrahedron Lett 1989;30:2493.
12. Creary X, Butchko MA. J. Org. Chem 2002;67:112. [PubMed: 11777447]
13. For selected examples of DFT studies in Au-chemistry, see: (a) Nevado C, Echavarren AM. Chem. Eur. J 2005;11:3155. (b) Comas-Vives A, González-Arellano C, Corma A, Iglisias M, Sánchez F, Ujaque G. J. Am. Chem. Soc 2006;128:4756. [PubMed: 16594712] (c) Nieto-Oberhuber C, López S, Muñoz MP, Cárdenas DJ, Buñuel E, Nevado C, Echavarren AM. Angew. Chem., Int. Ed 2005;44:6146. (d) Faza ON, López CS, Álvarez R, de Lera AR. J. Am. Chem. Soc 2006;128:2434. [PubMed: 16478199] (e) Straub BF. Chem. Commun 2004:1726. (f) Correa A, Marion N, Fensterbank L, Malacria M, Nolan SP, Cavallo L. Angew. Chem., Int. Ed 2008;47:718. (g) Nieto-Oberhuber C, Muñoz MP, Buñuel E, Nevado C, Cárdenas DJ, Echavarren AM. Angew. Chem., Int. Ed 2004;43:2402. (h) Shi F-Q, Li X, Xia Y, Zhang L, Yu Z-X. J. Am. Chem. Soc 2007;129:15503. [PubMed: 18027935] (i) Lemière G, Gandon V, Cariou K, Hours A, Fukuyama T, Dhimane A-L, Fensterbank L, Malacria M. J. Am. Chem. Soc 2009;131:2993. [PubMed: 19209868] (j) Nieto-Oberhuber C, Pérez-Galán P, Herrero-Gómez E, Lauterbach T, Rodríguez C, López S, Bour C, Rosellón A, Cárdenas DJ, Echavarren AM. J. Am. Chem. Soc 2008;130:269. [PubMed: 18076170]
14. B3LYP/6-31G*(LANL2DZ for Au) method was used for all the calculations, and solvation effect was calculated by CPCM model.
15. See Supporting Information for details.
16. (a) Sheng H, Lin S, Huang Y. Synthesis 1987:1022. (b) Fukuda Y, Shiragami H, Utimoto K, Nozaki H. J. Org. Chem 1991;56:5816. (c) Shapiro ND, Toste FD. J. Am. Chem. Soc 2007;129:4160. [PubMed: 17371031] (d) Wang W, Xu B, Hammond GB. J. Org. Chem 2009;74:1640. [PubMed: 19170532]

17. For examples of the proposed β-electrophilic attack on vinyl-gold, see: (a) Huang X, Zhang L. J. Am. Chem. Soc 2007;129:6398. [PubMed: 17472387] (b) Luzung MR, Mauleón P, Toste FD. J. Am. Chem. Soc 2007;129:12402. [PubMed: 17887681]

18. For review on counterion effects in Au-catalysis, see: (a) Gorin DJ, Sherry BD, Toste FD. Chem. Rev 2008;108:3351. [PubMed: 18652511] For selected examples, see: (b) Lemière G, Gandon V, Agenet N, Goddard J-P, de Kozak A, Aubert C, Fensterbank L, Malacria M. Angew. Chem., Int. Ed 2006;45:7596. (c) Bhunia S, Liu R-S. J. Am. Chem. Soc 2008;130:16488. [PubMed: 19554723] (d) Gorin DG, Watson IDG, Toste FD. J. Am. Chem. Soc 2008;130:3736. [PubMed: 18321110] (e) Kovács G, Ujaque G, Lledós A. J. Am. Chem. Soc 2008;130:853. [PubMed: 18166047]

19. Simulation of a base in the Ph_3AuOTf-catalyzed transformation using water cluster demonstrated that the 5-*endo-dig* cyclization path has the lowest energy profile, similarly to that for TfO^--counterion base. See Supporting Information for details.

20. For a single example of a solvent effect in the Au-catalyzed synthesis of pyrroles, see ref. [7i].

21. For review on silylfurans, see: Keay BA. Chem. Soc. Rev 1999;28:209.

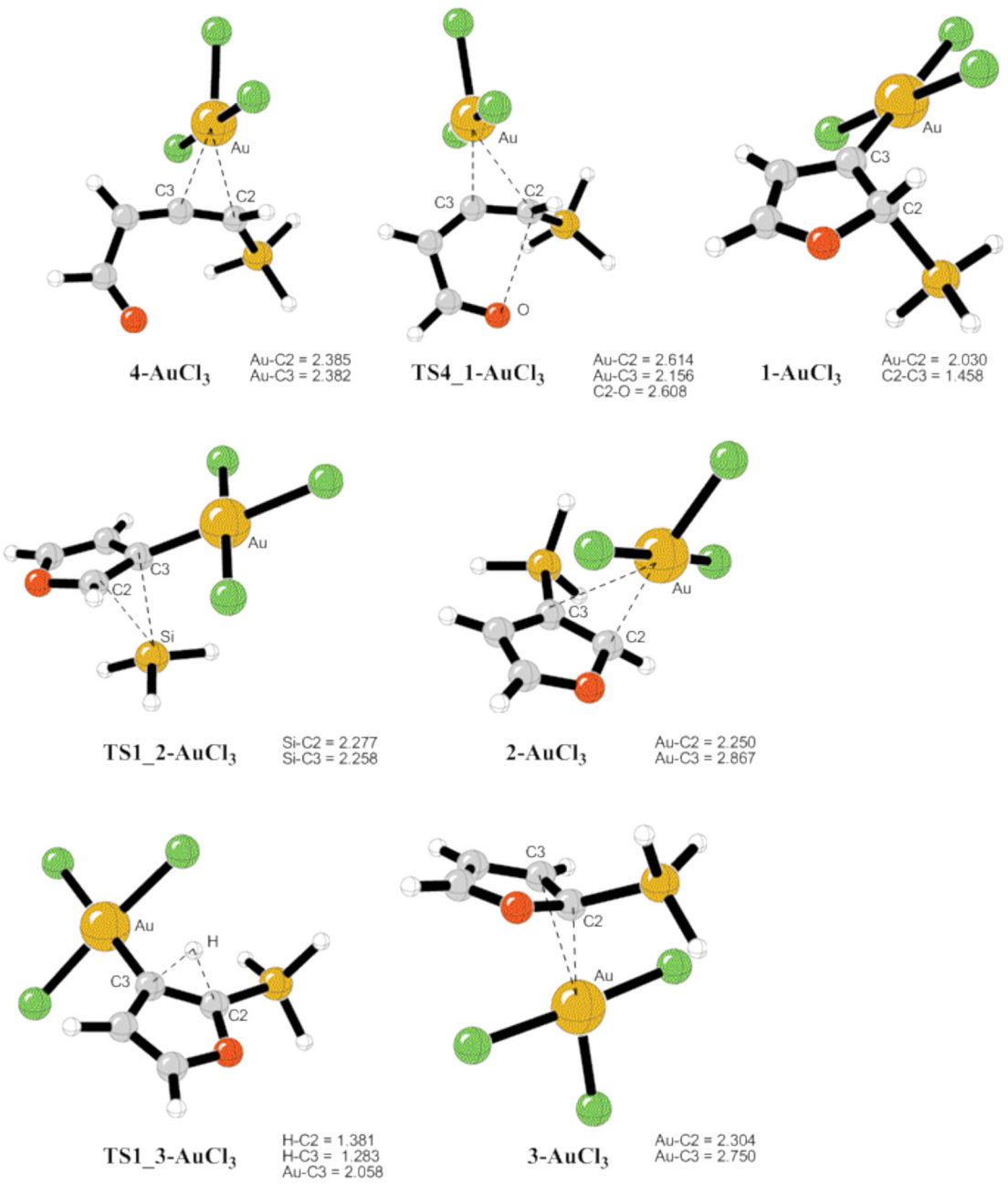

Figure 1.
Geometries for the intermediates and transition states given in Scheme 4, selected distances are in angstroms

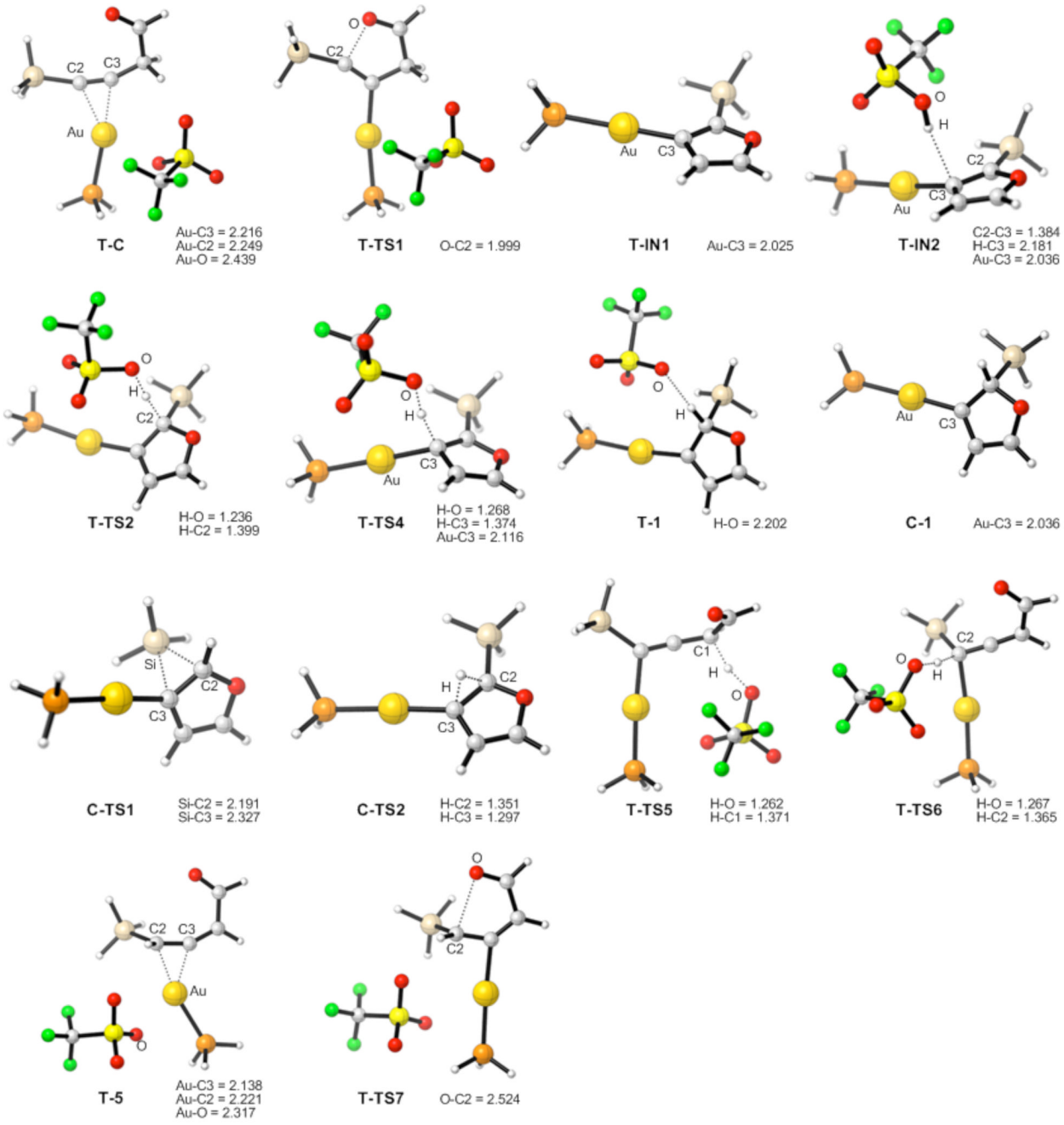

Figure 2.
Geometries of the intermediates and transition states for the $Ph_3PAuOTf$-catalyzed reaction, selected distances are in angstroms

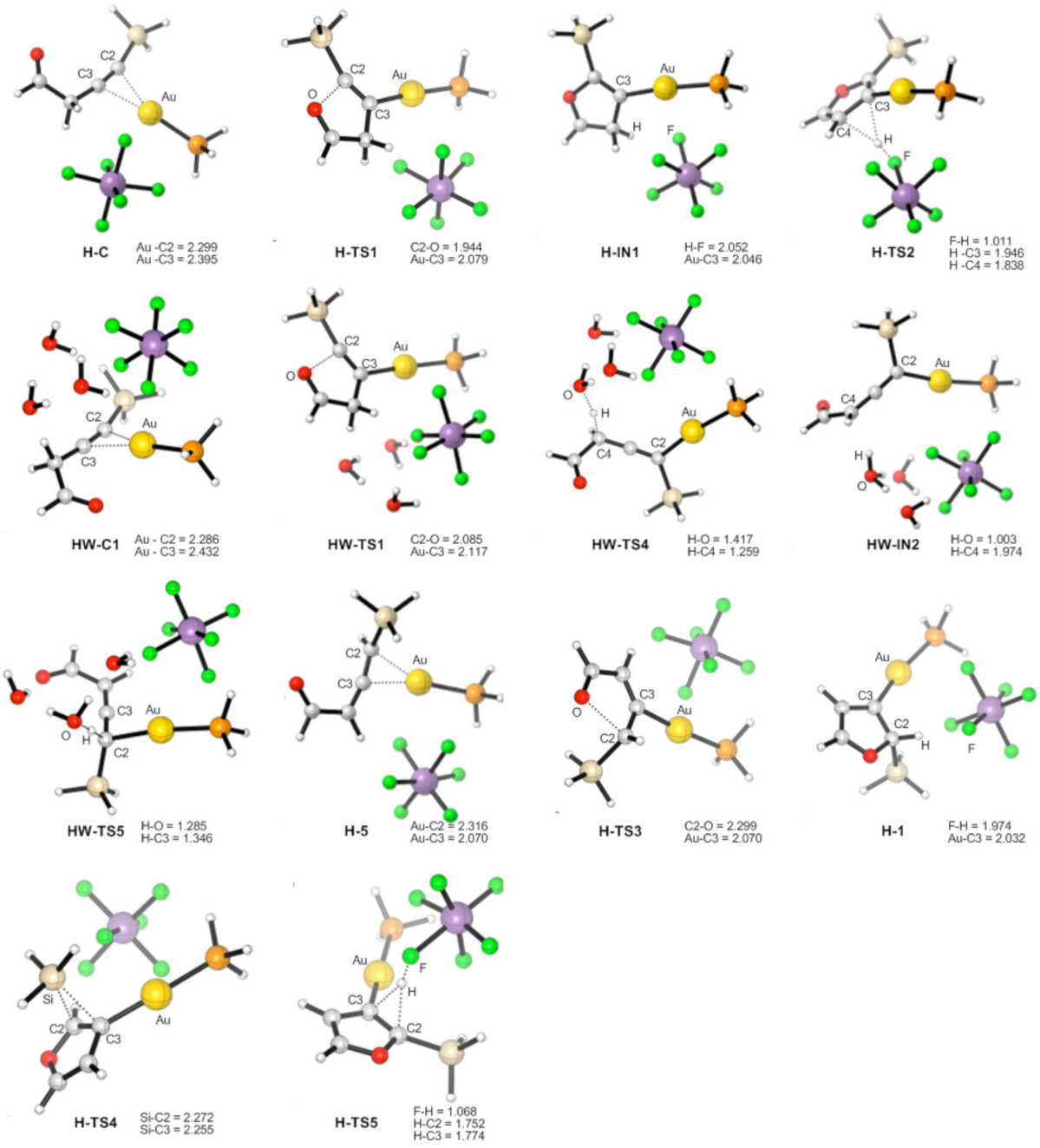

Figure 3.
Geometries of the intermediates and transition states for the $Ph_3PAuSbF_6$-catalyzed reaction, selected distances are in angstroms

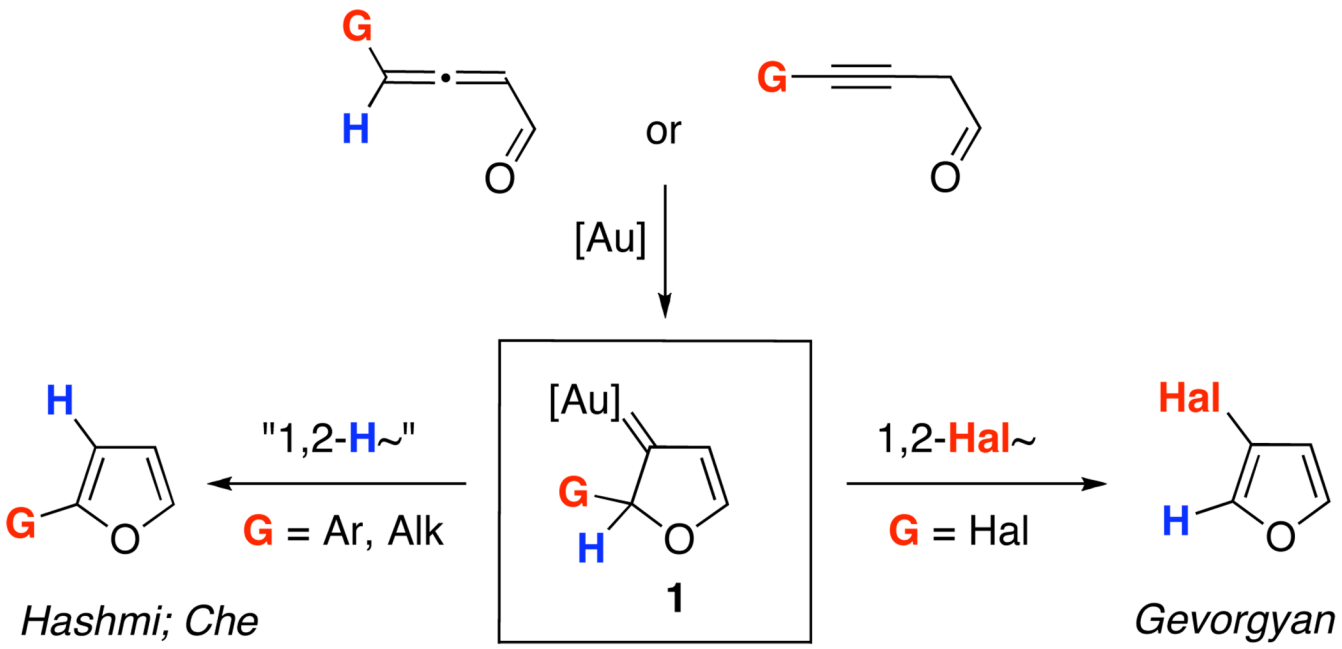

Scheme 1.
1,2-Group Migrations in the Synthesis of Furans via Au-Carbene Intermediate **1**

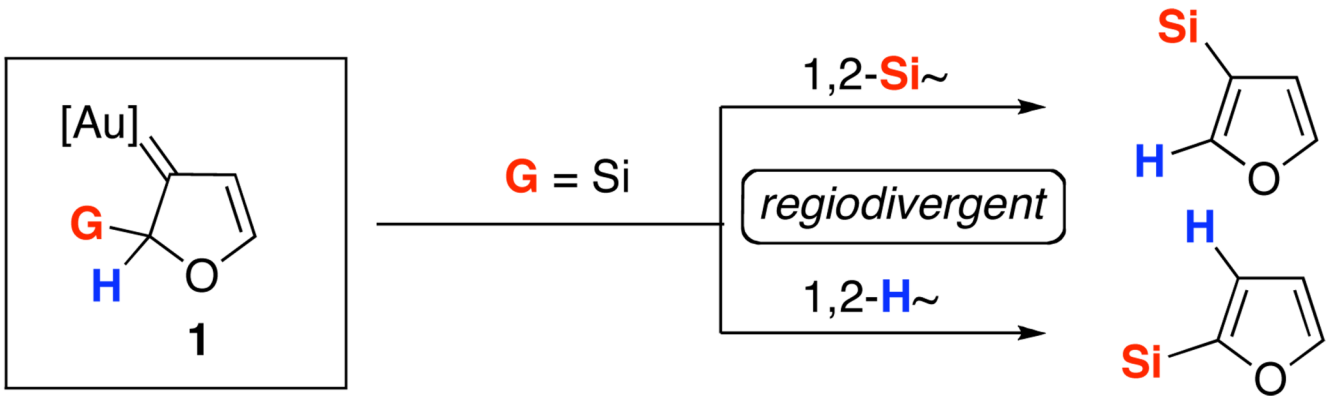

Scheme 2.
Regiodivergent 1,2-Si Migrations in the Synthesis of Furans via Au-Carbene Intermediate

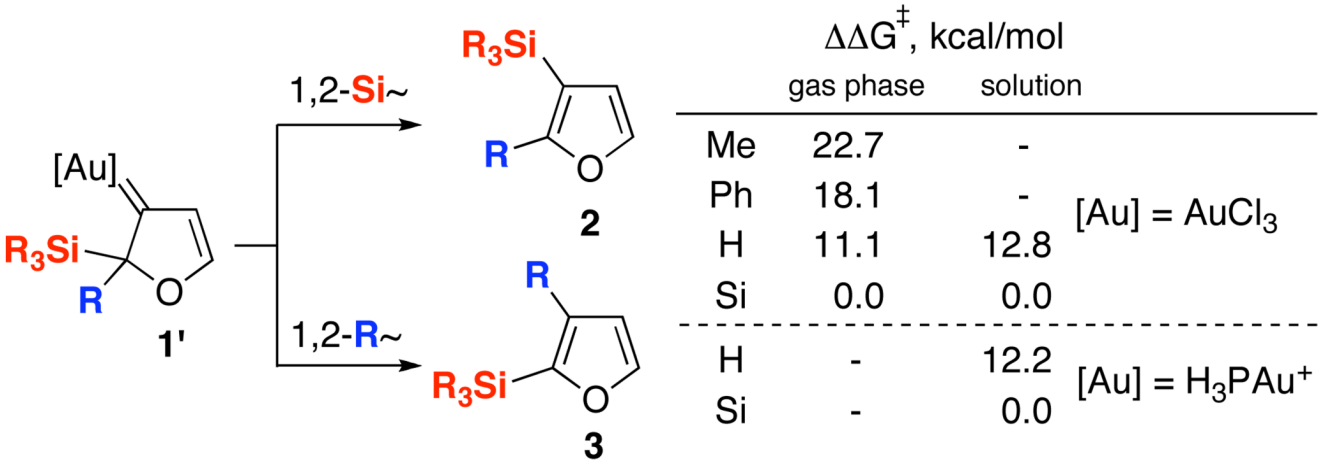

Scheme 3.
Predicted Activation Energies for the 1,2-Si- versus 1,2-R Migration in the Au-Carbene Intermediate **1'**

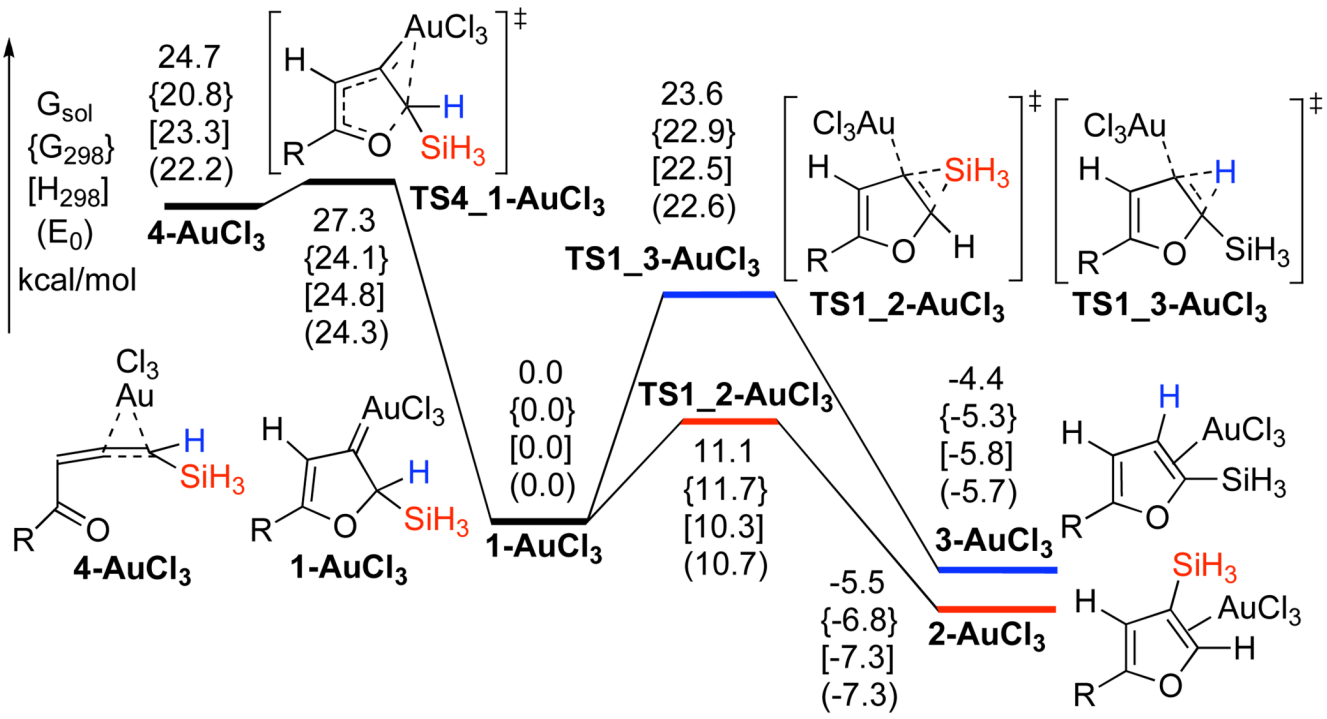

Scheme 4.

Potential Energy Surfaces for the $AuCl_3$-catalyzed Cycloisomerization of Allenes **4** (R = H)

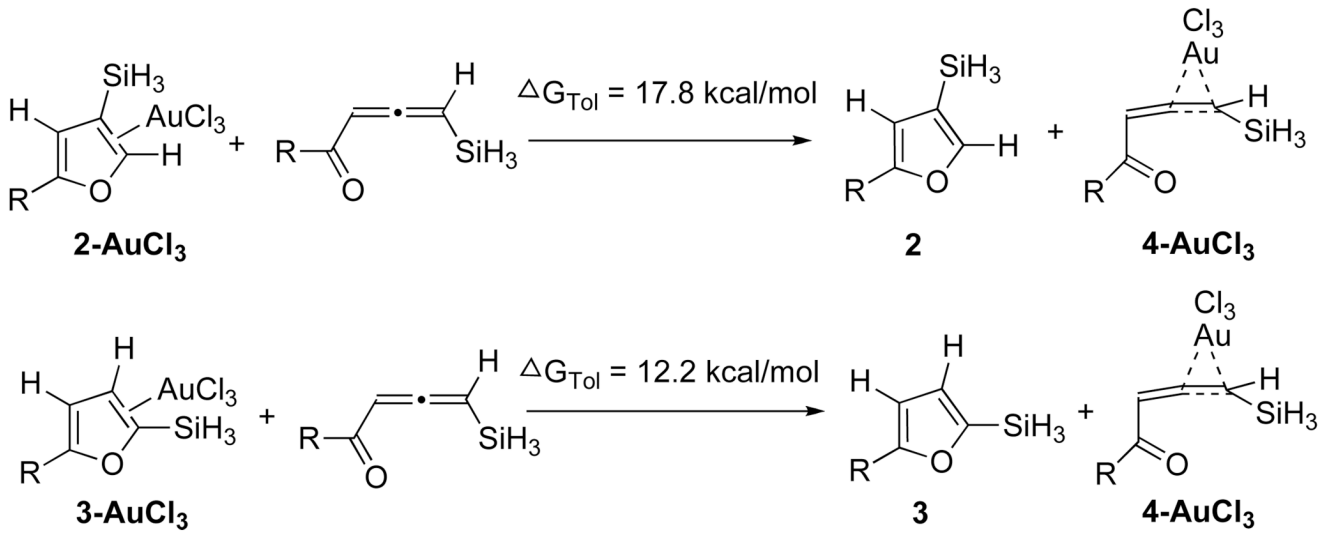

Scheme 5.
Generation of Products **2** and **3** from Complexes **2-AuCl$_3$** and **3-AuCl$_3$**

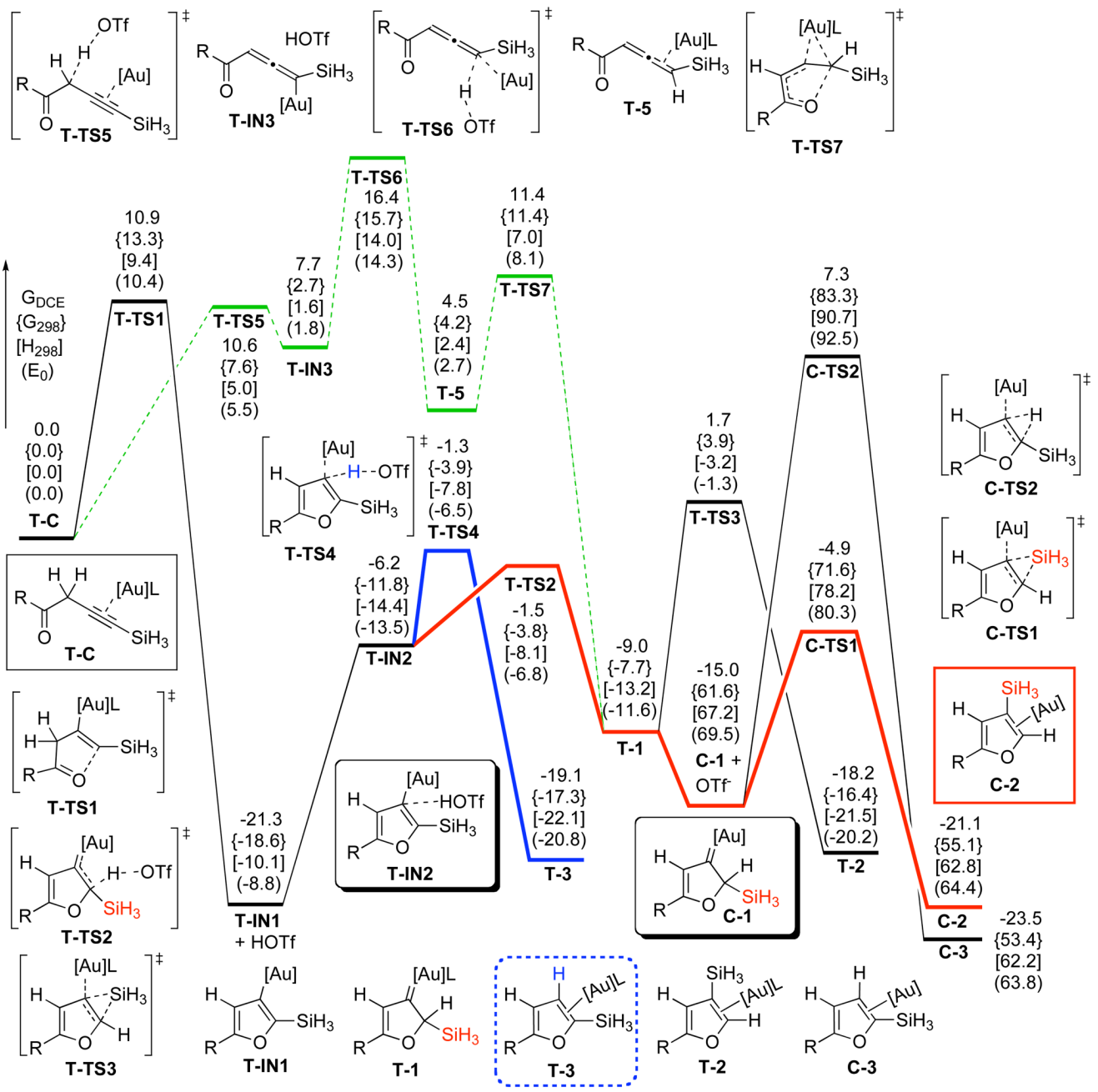

Scheme 6.

DFT Predictions for the $Ph_3PAuOTf$-Catalyzed Reaction ([Au] = $AuPH_3$, L = OTf, R = H) in 1,2-Dichloroethane Solution, Relative Energies (ΔG_{DCE}, ΔG_{298}, ΔH_{298}, ΔE_0) are in kcal/mol

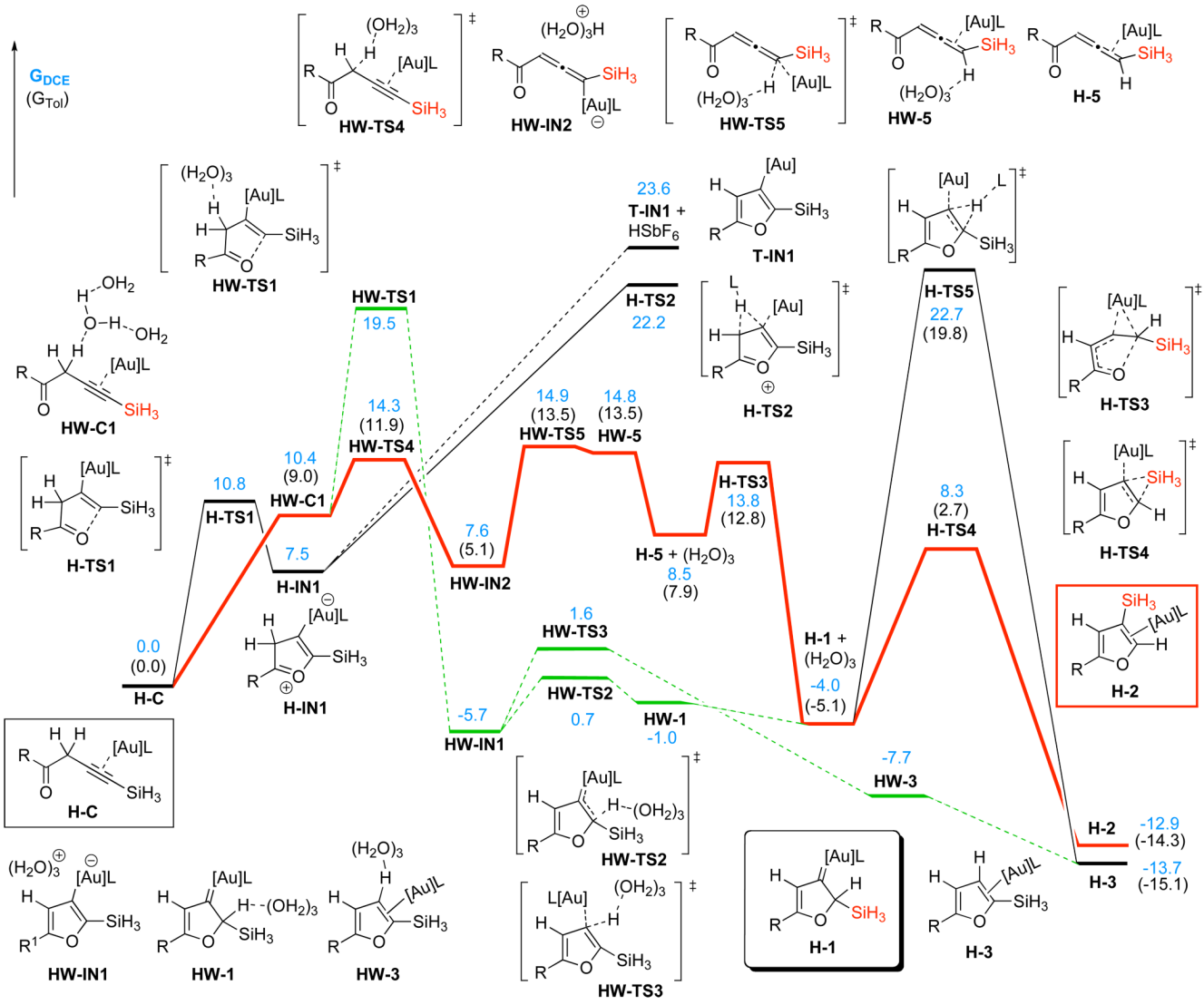

Scheme 7.

DFT Predictions for the $Ph_3PAuSbF_6$-Catalyzed Reaction ([Au] = $AuPH_3$, L = SbF_6, R = H) in 1,2-Dichloroethane and Toluene Solutions, Relative Energies (ΔG_{DCE}, ΔG_{Tol}) are in kcal/mol

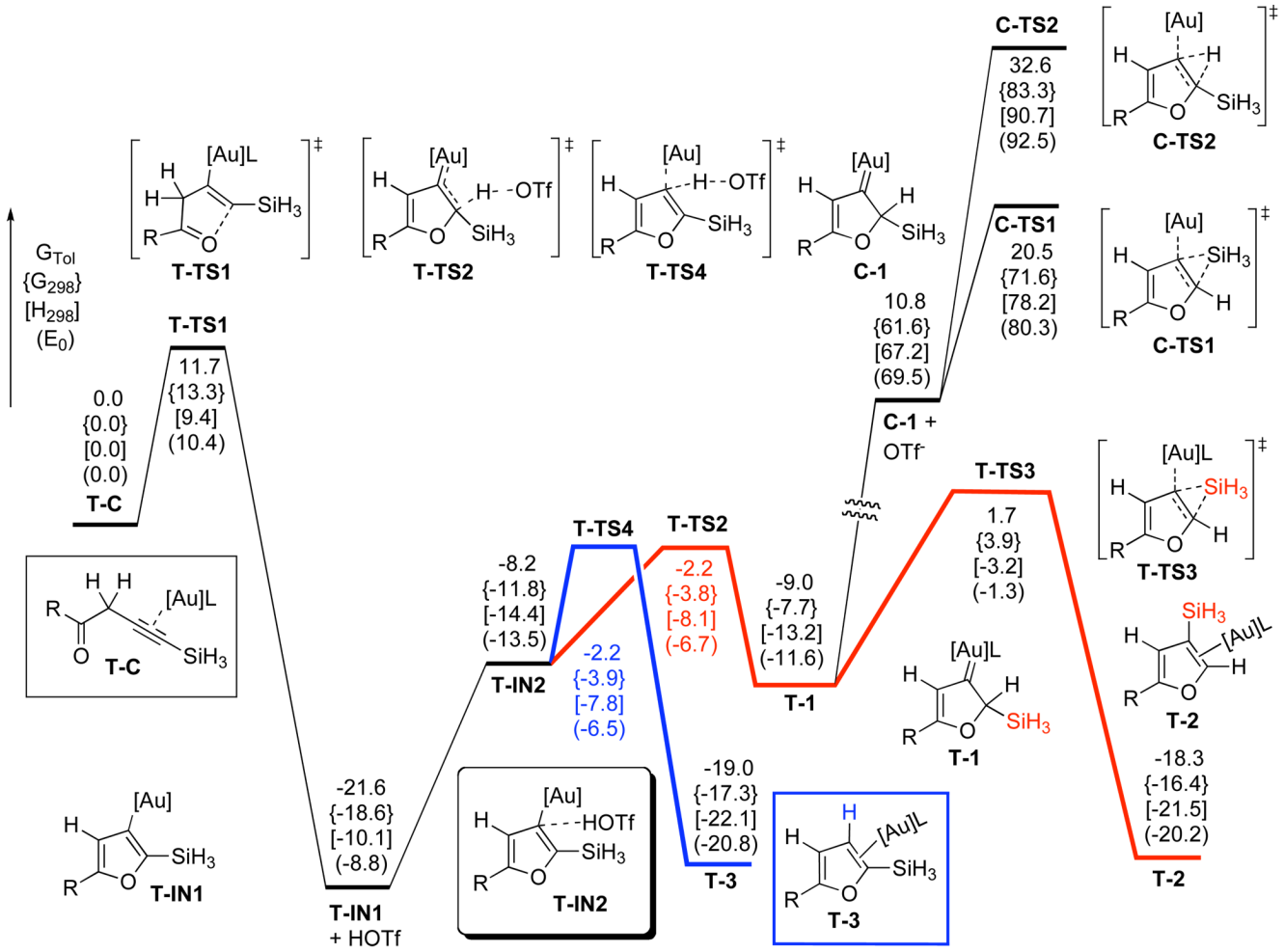

Scheme 8.

Solvation Effect of Toluene on the $Ph_3PAuOTf$-Catalyzed Reaction (R = H), Relative Free Energies in Toluene (ΔG_{Tol}) are in kcal/mol

Table 1

Au-Catalyzed Cycloisomerization of Allenyl Ketones **4**

5 mol %

0.5M in

Entry	Substrate
1	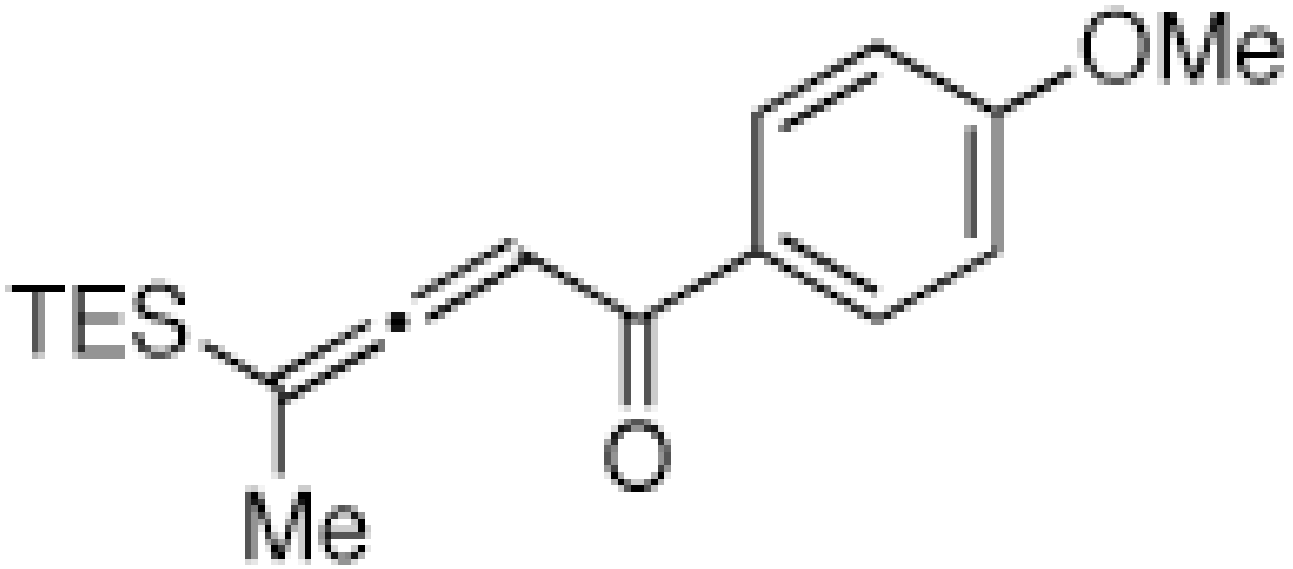
2	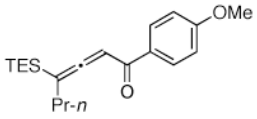

5 mol %

0.5M in

Entry	Substrate
3	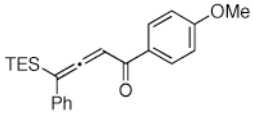
4	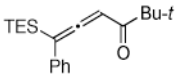
5	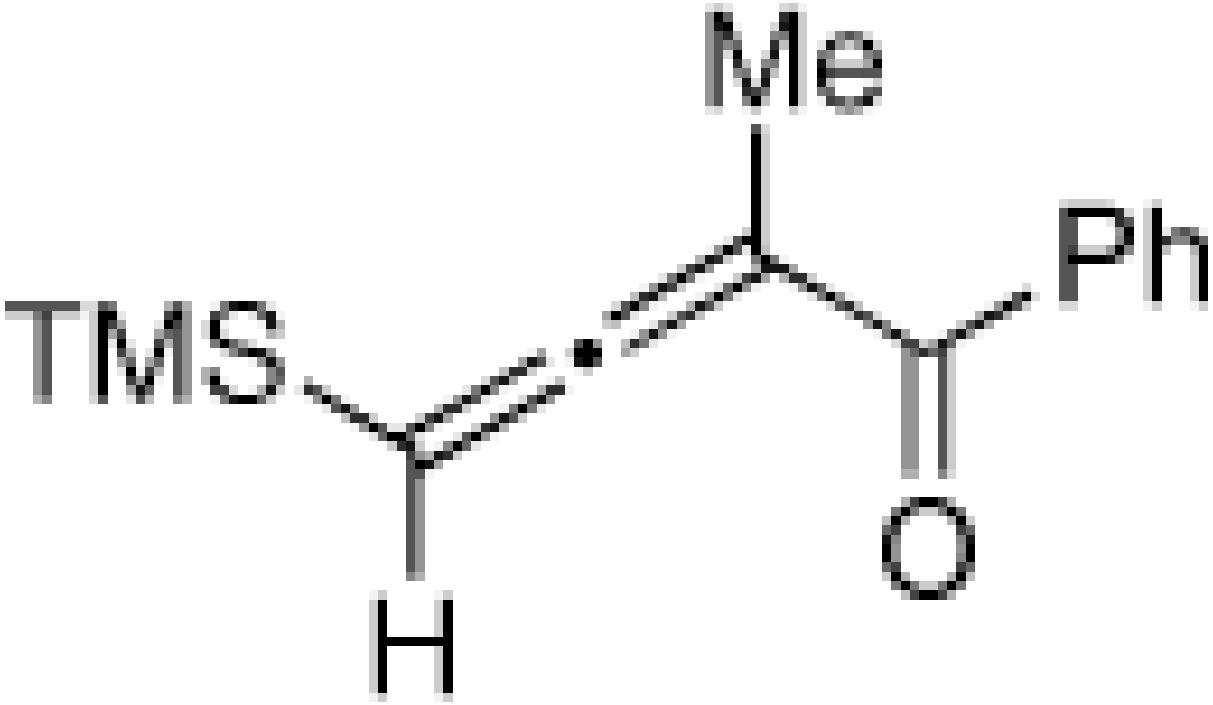

[a] Isolated yield of product for reactions performed on 0.5 mmol scale.

[b] Isolated yield of **2e** for reaction performed in $MeNO_2$.

[c] Isolated yield of **2e** for reaction performed with 1 mol % of catalyst.

Table 2

Optimization of the Au-Catalyzed Cycloisomerization of Homopropargyl Ketones **6**

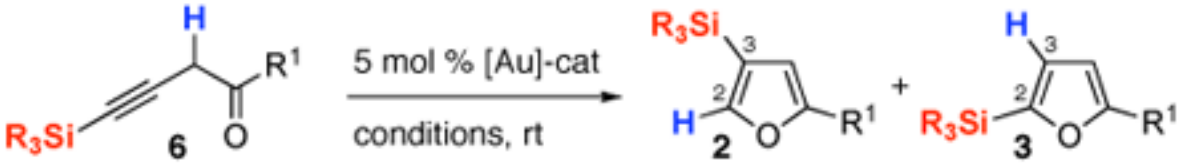

Entry	R^1	Catalyst	Solvent (C, M)	2 : 3 Ratio[a]
1	Ph (**6f**)	$Ph_3PAuSbF_6$	DCE (0.05)	100 : 0
2		$Ph_3PAuOTf$	DCE (0.05)	66 : 34
3		$Ph_3PAuOTf$	PhMe (0.1)	7 : 93
4		$AuCl_3$	PhMe (0.1)	60 : 40
5		$AuCl_3$	DCE (0.1)	72 : 28
6		$AuCl_3$	$MeNO_2$ (0.05)	84 : 16
7	*n*-C_8H_{17} (**6l**)	$Ph_3PAuSbF_6$	DCE (0.05)	100 : 0
8		$Ph_3PAuSbF_6$	PhMe (0.05)	100 : 0
9		$Ph_3PAuOTf$	PhMe (0.1)	12 : 88
10		$Ph_3PAuOTf$	DCE (0.05)	98 : 2
11	*t*-Bu (**6k**)	$Ph_3PAuSbF_6$	DCE (0.05)	100 : 0
12		$Ph_3PAuOTf$	PhMe (0.1)	17 : 83

[a] H^1 NMR ratio of products for reactions performed on 0.5 mmol scale.

Table 3

Au-Catalyzed Cycloisomerization of Homopropargyl Ketones **6**

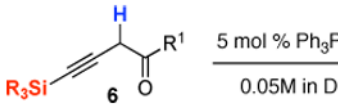

Entry	Substrate	Produ
1	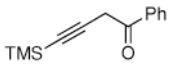	
2	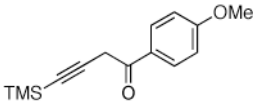	

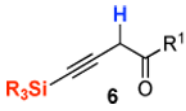

5 mol % Ph_3P

0.05M in D

Entry	Substrate	Produ
3	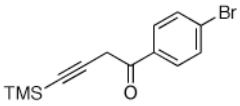	
4	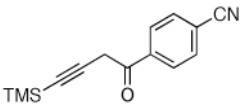	

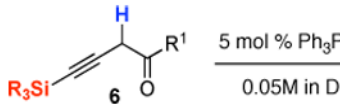

Entry	Substrate	Prod
5	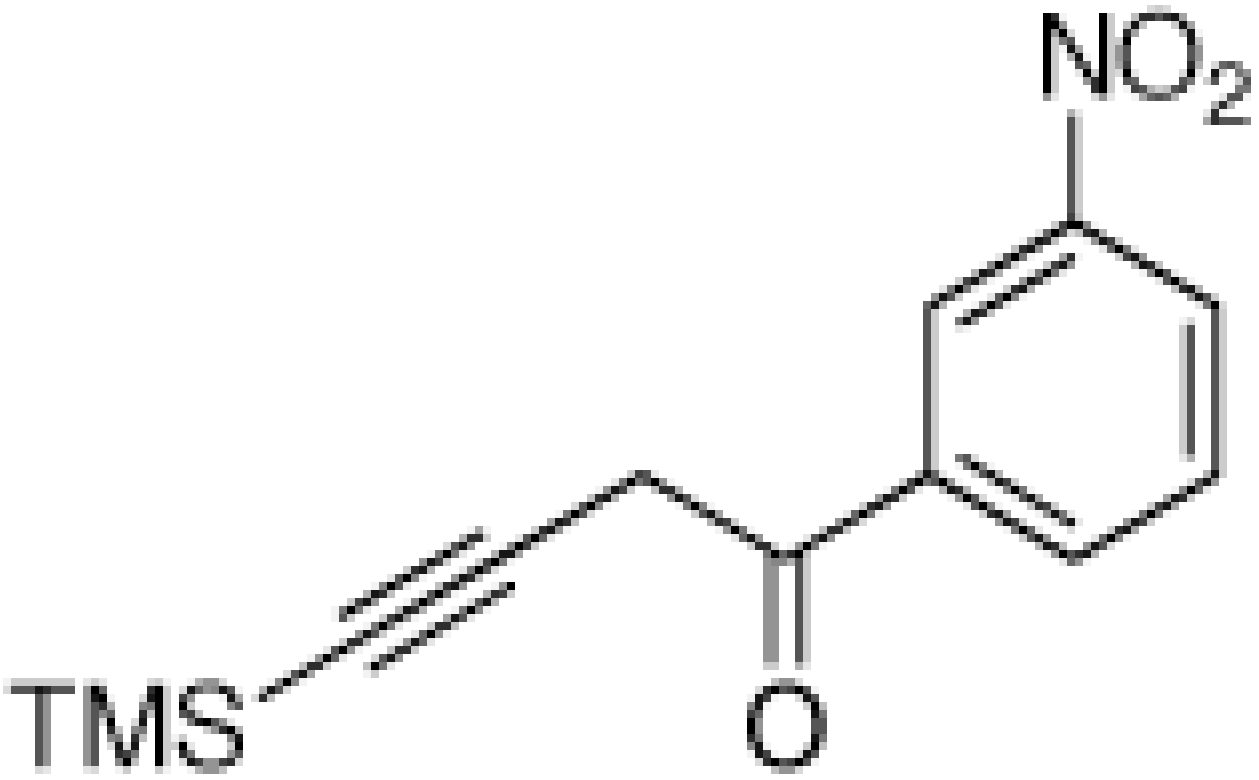	TMS H

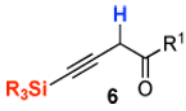

5 mol % Ph_3P

0.05M in D

Entry	Substrate	Prod
6		
7	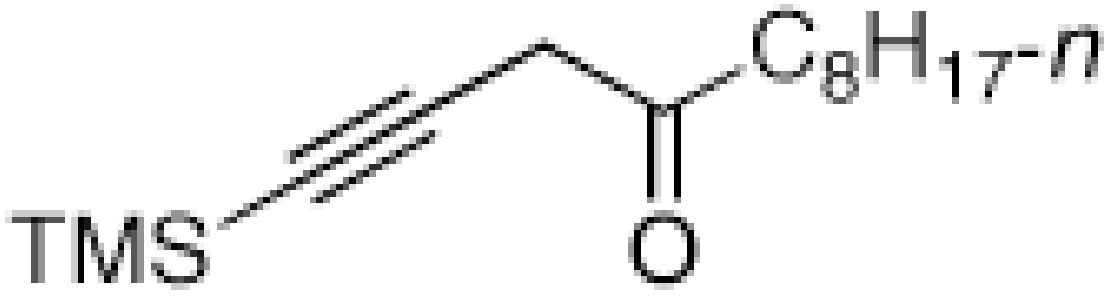	

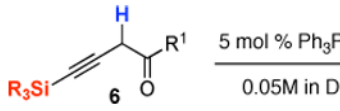

Entry	Substrate	Prod
8	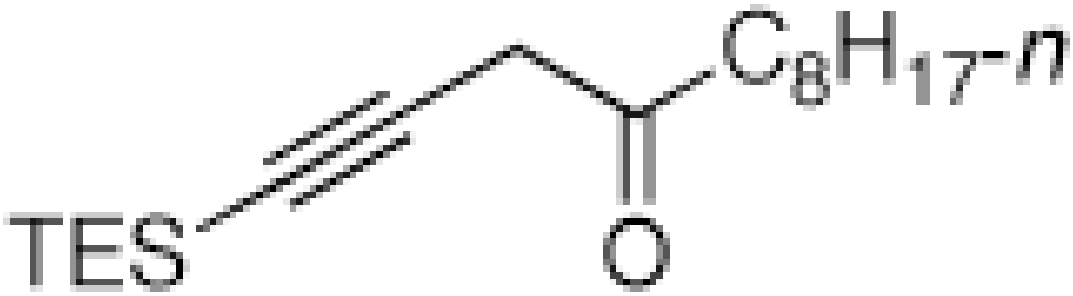	
9		

[a] Isolated yield of product for reactions performed on 0.5 mmol scale.

[b] **2f** and **2l** contained 8 and 6% of the corresponding desilylated furan, respectively.

[c] 14:1 ratio of **2h:3h**.

[d] 10:1 ratio of **2i:3i**.

[e] 8:1 ratio of **2j:3j**.

[f] GC Yield, **2k** is a volatile compound.